AFRL-RV-PS-TP-2012-0004

AFRL-RV-PS-TP-2012-0004

PERIODIC STRUCTURES IN THE EQUATORIAL IONOSPHERE (POSTPRINT)

Cheryl Y. Huang, et al.

13 May 2012

Interim Report

APPROVED FOR PUBLIC RELEASE; DISTRIBUTION IS UNLIMITED.

AIR FORCE RESEARCH LABORATORY
Space Vehicles Directorate
3550 Aberdeen Ave SE
AIR FORCE MATERIEL COMMAND
KIRTLAND AIR FORCE BASE, NM 87117-5776

REPORT DOCUMENTATION PAGE

Form Approved
OMB No. 0704-0188

1. REPORT DATE *(DD-MM-YYYY)*
13-05-2012

2. REPORT TYPE
Interim Report

3. DATES COVERED *(From - To)*
01 Oct 2008 – 25 Mar 2011

4. TITLE AND SUBTITLE
Periodic Structures in the Equatorial Ionosphere (Postprint)

5a. CONTRACT NUMBER

5b. GRANT NUMBER

5c. PROGRAM ELEMENT NUMBER
61102F

6. AUTHOR(S)
Cheryl Y. Huang, Susan H. Delay, Patrick A. Roddy, and Eric K. Sutton

5d. PROJECT NUMBER
2301

5e. TASK NUMBER
PPM00005202

5f. WORK UNIT NUMBER
EF004378

7. PERFORMING ORGANIZATION NAME(S) AND ADDRESS(ES)
Air Force Research Laboratory
Space Vehicles Directorate
3550 Aberdeen Ave. SE
Kirtland AFB, NM 87117-5776

8. PERFORMING ORGANIZATION REPORT NUMBER
AFRL-RV-PS-TP-2012-0004

9. SPONSORING / MONITORING AGENCY NAME(S) AND ADDRESS(ES)

10. SPONSOR/MONITOR'S ACRONYM(S)
AFRL/RVBXP

11. SPONSOR/MONITOR'S REPORT NUMBER(S)

12. DISTRIBUTION / AVAILABILITY STATEMENT
Approved for public release; distribution is unlimited. (377ABW-2011-1426 dtd 27 Sep 2011)

13. SUPPLEMENTARY NOTES
Radio Science, Vol. 46, RS0D14, doi:10.1029/2010RS004569, 2011. Government Purpose Rights.

14. ABSTRACT
The plasma densities detected by the Planar Langmuir Probe (PLP) on board the Communication/Navigation Outage Forecasting System (C/NOFS) satellite have been analyzed for the June 2008 period. This interval, which corresponds to one of the quietest periods in the space era, exhibited broad plasma decreases (BPDs) which we have reported previously. In order to treat the data quantitatively, we have detrended the PLP data by using the International Reference Ionosphere model to remove variations in density due to changes in spacecraft altitude and latitude along the orbit. In this paper we present results of a statistical analysis of C/NOFS detrended plasma densities during June 2008 as well as neutral densities from the Gravity Recovery and Climate Experiment measured during the same period. The results show periodic structures in both charged and neutral species, most evident in limited local times. These structures resemble wave-4 nonmigrating tides. BPDs persist in the detrended data and appear as one of the minima in the periodic signatures, most strikingly on the nightside.

15. SUBJECT TERMS
C/NOFS, Planar Langmuir Probe, broad plasma decreases, plasma densities

16. SECURITY CLASSIFICATION OF: a. REPORT	b. ABSTRACT	c. THIS PAGE	17. LIMITATION OF ABSTRACT	18. NUMBER OF PAGES	19a. NAME OF RESPONSIBLE PERSON
Unclassified	Unclassified	Unclassified	Unlimited	12	Cheryl Huang
					19b. TELEPHONE NUMBER *(include area code)*

Standard Form 298 (Rev. 8-98)
Prescribed by ANSI Std. 239.18

RADIO SCIENCE, VOL. 46, RS0D14, doi:10.1029/2010RS004569, 2011

Periodic structures in the equatorial ionosphere

Cheryl Y. Huang,[1] Susan H. Delay,[2] Patrick A. Roddy,[1] and Eric K. Sutton[1]

Received 29 November 2010; revised 25 March 2011; accepted 20 May 2011; published 3 August 2011.

[1] The plasma densities detected by the Planar Langmuir Probe (PLP) on board the Communication/Navigation Outage Forecasting System (C/NOFS) satellite have been analyzed for the June 2008 period. This interval, which corresponds to one of the quietest periods in the space era, exhibited broad plasma decreases (BPDs) which we have reported previously. In order to treat the data quantitatively, we have detrended the PLP data by using the International Reference Ionosphere model to remove variations in density due to changes in spacecraft altitude and latitude along the orbit. In this paper we present results of a statistical analysis of C/NOFS detrended plasma densities during June 2008 as well as neutral densities from the Gravity Recovery and Climate Experiment measured during the same period. The results show periodic structures in both charged and neutral species, most evident in limited local times. These structures resemble wave-4 nonmigrating tides. BPDs persist in the detrended data and appear as one of the minima in the periodic signatures, most strikingly on the nightside.

Citation: Huang, C. Y., S. H. Delay, P. A. Roddy, and E. K. Sutton (2011), Periodic structures in the equatorial ionosphere, *Radio Sci.*, *46*, RS0D14, doi:10.1029/2010RS004569.

1. Introduction

[2] It is generally accepted that the equatorial low-latitude ionosphere is influenced by solar radiation, magnetic activity and variations in solar cycle [*de La Beaujardière et al.*, 2004]. These combine to create a wealth of plasma interactions which reflect changes in local time, latitude, altitude and season. Extensive studies of plasma irregularities have established the complex relationship between *E* and *F* region electric fields and neutral winds driving the growth of the Rayleigh-Taylor instability [see *de La Beaujardière et al.*, 2004, and references therein]. The C/NOFS satellite was launched in April 2008 with the aim of predicting communications outages due to these equatorial irregularity structures.

[3] However more recent studies have indicated the importance of the troposphere as a contributor to ionospheric structure. Migrating and nonmigrating tides [*Chapman and Lindzen*, 1970] are caused by an interaction between tropospheric latent heat and solar diurnal tides which are generated by solar radiation [*Hagan and Forbes*, 2002, 2003]. Discovery that these tides penetrate deep into the upper *F* region was unexpected, as planetary waves are expected to damp out far below the *F* region peak. Results from the C/NOFS mission have confirmed that tidal structures are dominant in the ionosphere, being reported from a number of separate investigations over the entire altitude range of the satellite which extends to 800 km [*Pfaff et al.*, 2010; *Araujo-Pradere et al.*, 2010; *Dao et al.*, 2010]. In this paper we present an analysis of periodic structures resembling tides found in C/NOFS plasma densities, and focus on one particular phenomenon called a Broad Plasma Decrease (BPD).

[4] In our previous study [*Huang et al.*, 2009], we reported BPDs observed on C/NOFS as well as on the CHAllenging Minisatellite Payload (CHAMP) and Defense Meteorological Satellite Program (DMSP) satellites. An example of a BPD on C/NOFS is shown in Figure 1 which occurred on 5 June 2008, orbit 734. Figure 1 (top) shows the plasma density (1 min averages in black, 1 s averages in green) together with the satellite altitude (in blue, with heavier trace when the spacecraft is on the nightside). In this paper we refer only to the 1 min averages. Ephemeris information is given in the table at bottom. Figure 1 (middle) gives an indication of the frequency of the fluctuations, not referenced in this study. Figure 1 (bottom) shows the orbit in red, with a heavier trace showing when the satellite is on the nightside. Also shown in Figure 1 (bottom) is the magnetic equator in green. The large decrease in plasma density commencing at approximately 04:09 UT is the signature of the BPD. As noted in our past study, BPDs are a regular feature of solar minima, with the largest BPDs seen during the recent past solar minimum. They are most evident at South Atlantic Anomaly longitudes, although they are also detected in other longitude regions. In general BPDs are detected between May and July on DMSP in every solar minimum year in the 2006–2010 interval in the recent solar minimum, but also in 1996 in the previous solar minimum [*Huang et al.*, 2009]. In order to show BPDs together with periodic structures clearly, we restrict analysis in this paper to the June 2008 period, although they also occur in June 2009–2010.

[5] Quantitative analysis of these density variations is made difficult by the changes in C/NOFS location. Note that from the start of the density decrease shown in Figure 1 to the end, the satellite altitude changes from approximately

[1]Space Vehicles Directorate, Air Force Research Laboratory, Hanscom AFB, Massachusetts, USA.
[2]Institute for Scientific Research, Boston College, Chestnut Hill, Massachusetts, USA.

0048-6604/11/2010RS004569

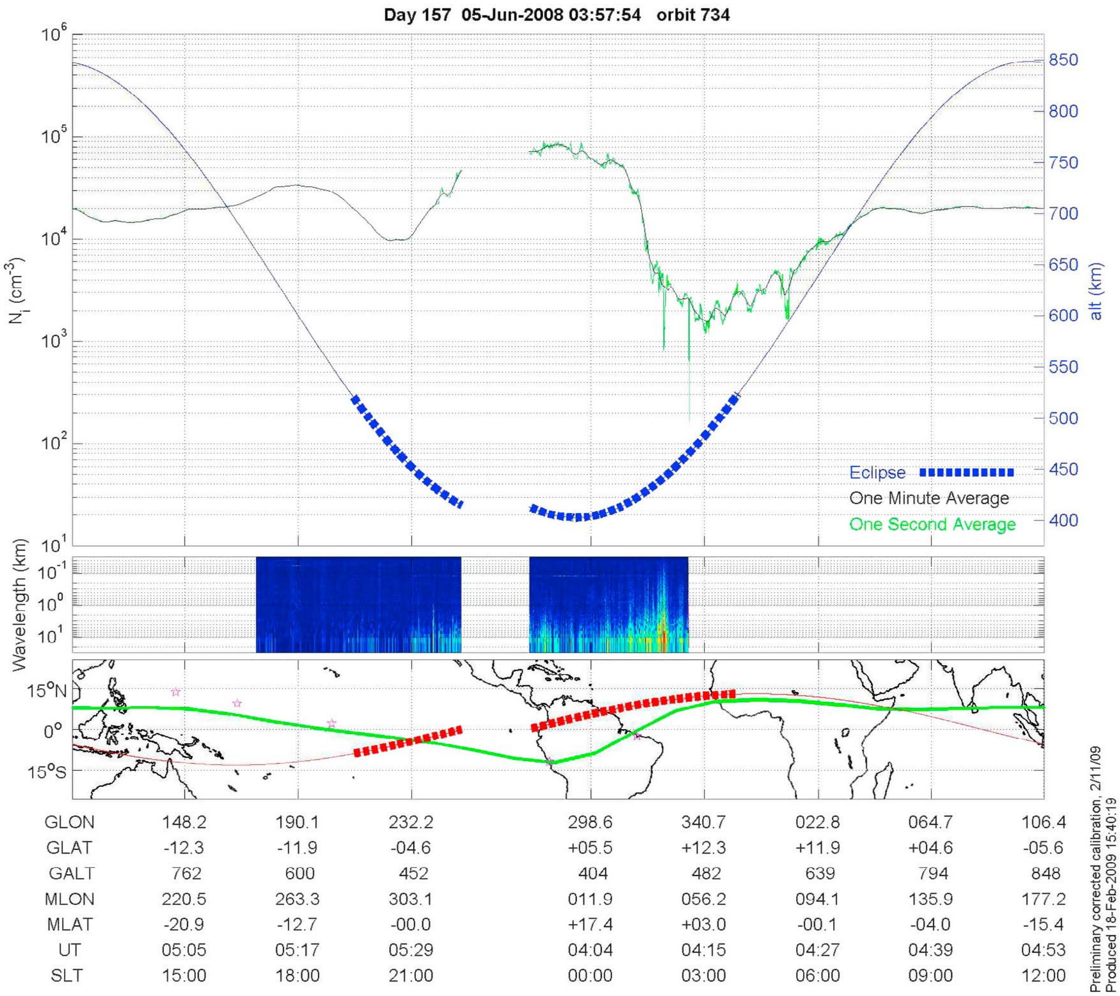

Figure 1. C/NOFS observations of a Broad Plasma Depletion (BPD) on 5 June 2008. (top) The plasma density (black line) in 1 min resolution as well as 1 s resolution (green line). C/NOFS altitude is indicated by the blue line, with the heavy dotted section showing when the satellite is in darkness. (middle) The spectrum of the high time resolution density fluctuations. (bottom) The magnetic equator is shown by a green trace, and satellite orbit is indicated by the red trace, with the heavy dotted section indicating when the spacecraft is in darkness. The BPD starts at 04:09 UT, with recovery after 04:33 UT. Ephemeris information is given along the bottom.

400 km at 04:09 UT to 700 km at 04:33 UT. In order to reduce the density variations due to change in satellite altitude and latitude we have detrended the plasma data by using the IRI model. Altitude is the main contributor to orbital variations, hence we refer to our detrending process as altitude-detrending for clarity. The data are all referenced to the equator at an altitude of 500 km. We then analyze the altitude-detrended data in order to quantify the density variations. The focus in this paper is on the June 2008 period. This period is marked by extremely quiet magnetic conditions, with solar UV fluxes the lowest seen for many decades. There are high-speed streams in the solar wind which affect the ionosphere and thermosphere periodically, but not daily. BPDs are observed both in the presence and absence of fast streams. Without external driving by the solar wind, the ionosphere is affected strongly by internal processes.

[6] We carried out a statistical analysis on June 2008 accelerometer data from the GRACE satellite to determine if the structures that appeared in the plasma analysis were also present at the same time in the neutral densities. This appears to be the case, although the coupling between ions and neutrals is not straightforward.

2. Instrumentation

[7] The PLP on C/NOFS measures plasma densities, electron temperatures and density fluctuations at rates ranging from 32 to 1024 samples s^{-1}. We have used 1 min averaged data for our analysis. In this paper we focus on electron densities on the nightside. During June 2008, the period of this study, density depletions were observed over the full range of the C/NOFS orbit, from 400 to 840 km.

[8] Neutral densities on the Gravity Recovery and Climate Experiment (GRACE) satellite were measured using superSTAR accelerometers, using the techniques of *Sutton et al.* [2005] and *Sutton* [2009]. These measurements are similar to those made by the STAR accelerometer on

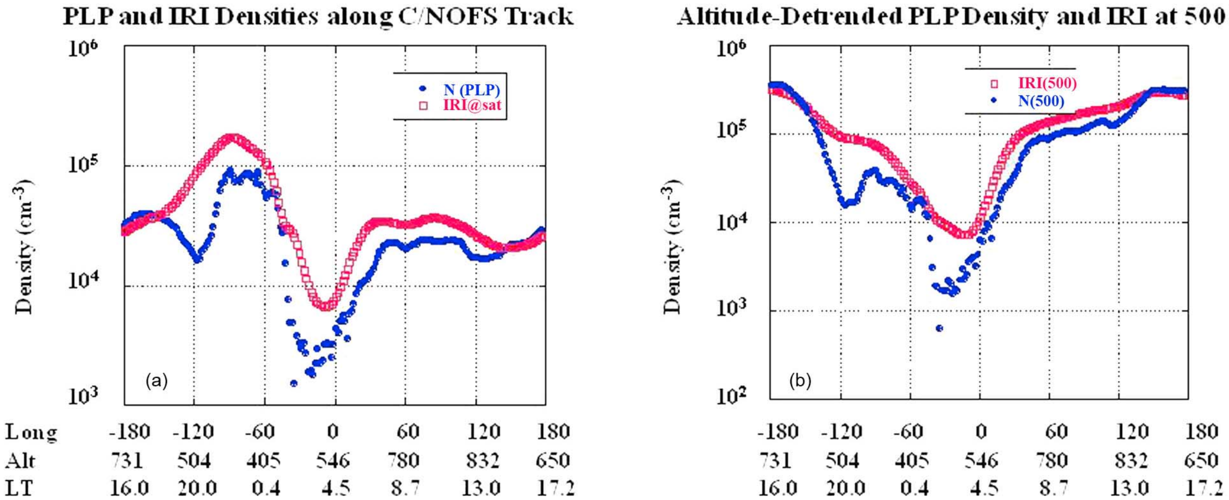

Figure 2. (a) The plasma density measured by the Planar Langmuir Probe (PLP) along the satellite track on 5 June 2008, orbits 733–734. The results are shown as functions of geographic longitude, altitude, and local time. Solid blue circles denote the PLP measurements. The values of the International Reference Ionosphere (IRI) model for the satellite location are indicated by red squares. (b) The result of altitude-detrending the PLP plasma density using the IRI model. Altitude-detrended and IRI plasma densities are shown at an altitude of 500 km and at the equator.

CHAMP [*Bruinsma et al.*, 2004; *Sutton*, 2009], with a precision an order of magnitude greater than the CHAMP instrument. In this study, 5 s data were used. During the period of interest, the satellite is in a 443 × 485 km orbit. Factoring in the oblateness of the Earth, the minimum altitude in the World Geodetic System 84 (WGS84) was 460 km and the maximum was 506 km.

[9] GRACE makes 30–32 equatorial passes per day; 15–16 on the ascending portion of its orbit and 15–16 on the descending. Given the rotation of the Earth, each of the passes occurs over a different longitude such that after a day, there are 15–16 data points equally spaced in longitude, per hemisphere. The repeat ground track period is 7 days, after which time there are about 112 data points equally spaced in longitude, per hemisphere. The GRACE plots in this paper use 28 days, so there are 4 repeat ground tracks in longitude, with limited coverage of local times. In this report we include only those local times for which we have sufficient numbers of observations. We restrict the data to the same latitude range as that covered by the C/NOFS satellite during June 2008.

3. Observations

[10] An example of the observations that stimulated this investigation is shown in Figure 1. As already noted, the BPD which spans 16 min from 04:09 UT to 04:25 UT is detected over an altitude range from 750 to 600 km. This spatial variation makes it difficult to evaluate the true reduction in density. In order to quantify the density decreases, we use the 2007 version of the IRI model [*Bilitza and Reinisch*, 2008] using the default topside density model. PLP densities are then processed as follows:

$$N_{Det} = N(PLP) * N(IRI \text{ at } 500 \text{ km})/N(IRI \text{ at } C/NOFS \text{ location}),$$

where N(PLP) is the density measured by PLP along the C/NOFS orbit; N(IRI at 500km) is the IRI value at the equator at 500 km altitude; and N(IRI at C/NOFS location) is the IRI value at the same location and local time as the PLP instrument.

[11] By taking the ratio of two IRI model values, we minimize the intrusion of the model in our altitude-detrending scheme. We treat all the altitude-detrended values as if measured at the equator at a constant height of 500 km. It should be noted that the very low ionospheric densities during June 2008 are not represented well by IRI. However, our detrending scheme does not rely on absolute values of density in the model, only on the relative densities at different altitudes.

[12] Figure 2 illustrates the altitude-detrended densities for parts of orbits 733 and 734 covering most of the interval shown in Figure 1. The plots show densities as functions of geographic longitude, altitude, and local time. Figure 2a shows the original densities along the C/NOFS orbit track, together with the IRI model values at the satellite location. Figure 2b shows the altitude-detrended densities together with the IRI model values at 500 km at the equator. Note that the scales on the two plots are different. Mapping PLP densities to 500 km extends the density range since the original orbit was close to apogee on the dayside. In Figure 2b the BPD can be seen between −40°W (or 320°E) longitude and about 20°E longitude. Note that there are other depletions evident in Figures 2a and 2b between −90°W and −150°W longitude. As we will show below, periodic modulations are strikingly in evidence during June, with the BPD the largest feature within the periodic structures.

[13] In the original data, the density decreased from 8×10^4 cm^{-3} at 04:06 UT (near satellite perigee at 400 km) to 1.8×10^3 cm^{-3} at 04:16 UT near our nominal altitude of 500 km. In the altitude-detrended data, the densities are 1.8×10^4 cm^{-3} and 1.7×10^3 cm^{-3} at the corresponding

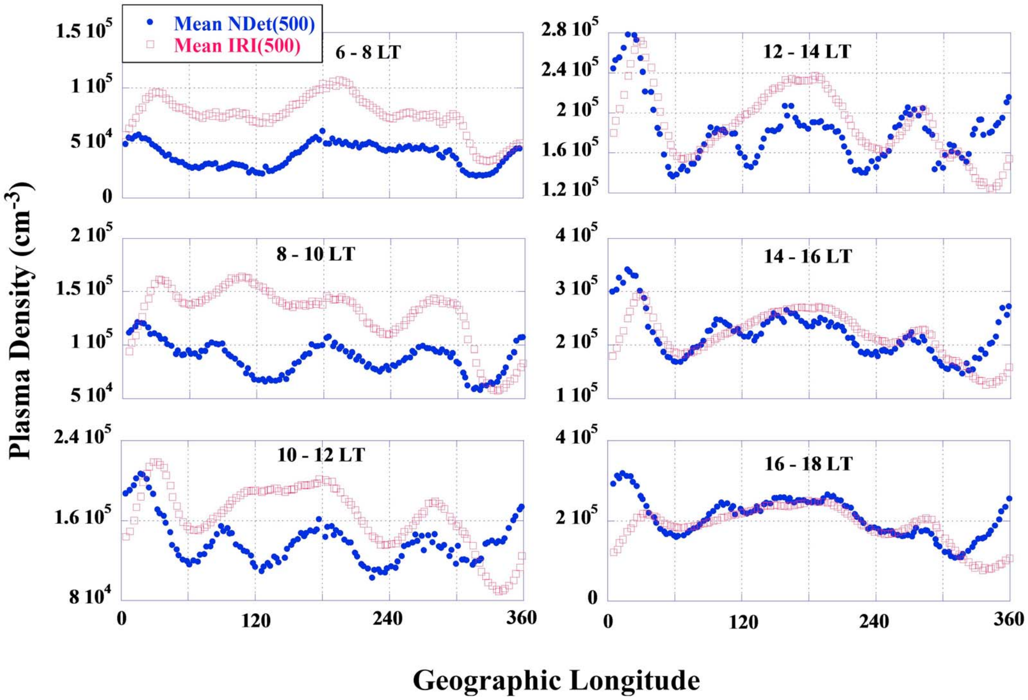

Figure 3. Altitude-detrended PLP plasma densities are shown as functions of longitude for the dayside, divided into 2 h local time averages. The data are averaged over 3° wide longitudinal bins. For comparison the IRI values are included. Wave-4 periodicity can be seen in the plots for 08:00–10:00 LT, 10:00–12:00 LT, and 12:00–14:00 LT. At dawn a two-wave structure can be observed.

times. The altitude-detrended density shows a decrease of 91% within the BPD while the original density decreases by 98%. Altitude variation obscures the "true" density change. In addition, altitude-detrending reveals density variations which are not as easy to identify as the BPD in Figure 1. These will become apparent in our statistical analysis. Also evident in Figure 2 are the differences between the measured plasma density during this extremely deep solar minimum and the IRI model values. This is not altogether unexpected given that solar flux values during 2008 are far below past solar minimum observations.

[14] Figures 3 and 4 show the average altitude-detrended densities, N_{Det} on the dayside and nightside, respectively, together with IRI model values for the month of June 2008. The densities have been sorted into 2 h local time bins and averaged over 3° of geographic longitude. The averages are shown as functions of longitude for each local time. Figure 3 (left) shows the results for 06:00–08:00 LT, 08:00–10:00 LT, and 10:00–12:00 LT. Figure 3 (right) shows results for 12:00–14:00 LT, 14:00–16:00 LT, and 16:00–18:00 LT. This is repeated in Figure 4 for local times on the nightside, as indicated in each panel. Although not shown in Figure 3 or Figure 4, the standard deviations of N_{Det} within each longitude bin can be large, at times comparable with the values themselves.

[15] The neutral densities derived from the GRACE accelerometer were analyzed to remove altitude and local time variations as follows. During an orbit, the near-polar inclination of the GRACE satellite allows for near-global latitudinal sampling. Each latitude is sampled twice during an orbit, at two different local times that are approximately 12 h apart. There are 15–16 satellite orbits per day, which provides full longitudinal coverage on the ascending and descending portions of the orbit. Therefore, an effective zonal mean density, ρ_{zm}, can be computed at each latitude and altitude for each day. This zonal mean can then be removed from the density data to yield a percent residual: $100*(\rho - \rho_{zm})/\rho_{zm}$. These residuals are binned according to latitude and longitude, for both ascending and descending portions of the orbit.

[16] The resulting plots show the longitudinal structure of the thermosphere as viewed from a satellite in a nearly fixed local time frame. Longitudinal structures of a certain wave number, k, should be interpreted as a sum of all of the tidal components with $|s - n| = k$, where $2\pi n$ is the frequency of oscillation (in days) and s is the zonal wave number from classical tidal theory [see *Lindzen and Chapman*, 1969].

[17] Two additional caveats arise from interpreting these plots. First, by removing the daily zonal mean density, the residuals alias with the migrating tides such that the residuals will be smaller when the satellite's orbital plane is in phase with the migrating tides, and larger when out of phase. In an effort to minimize this problem, we use both the ascending and descending density values to compute the daily zonal mean density for a set of data points at a given latitude. This removes the aliasing effects of the migrating tides with n = 1, 3, 5,…, while leaving the effects caused by the migrating tides with n = 2, 4,….

[18] The second caveat is that the different tidal modes can cancel one another depending on their phases and the local time of the satellite such that the observed amplitudes

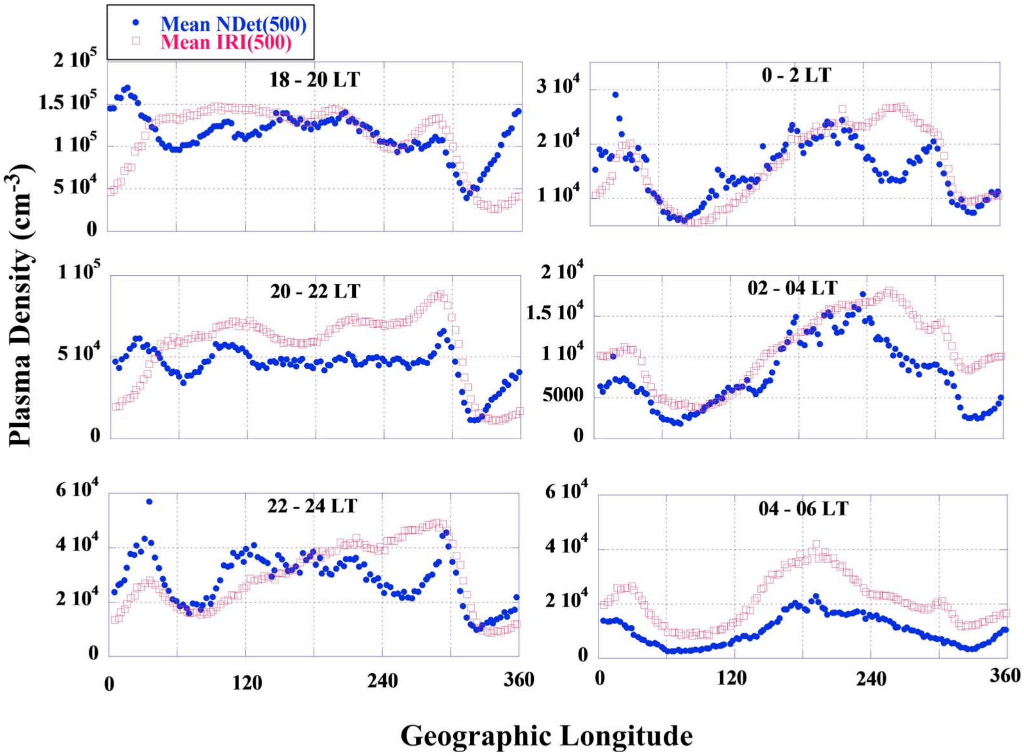

Figure 4. Altitude-detrended PLP plasma densities are shown as functions of longitude for the nightside, divided into 2 h local time averages. The data are averaged over 3° wide longitudinal bins. IRI model values are shown for comparison. For most of the night, there is much weaker evidence of wave-like structure, except near dawn where a two-wave periodicity can be seen. Deep density minima in the 300°–360° longitude sector can be seen in all the plots, most clearly in the 20:00–22:00 LT sector.

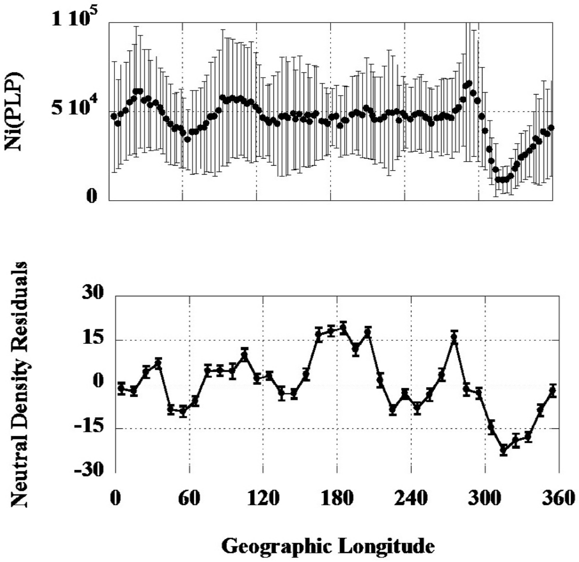

Figure 5. Altitude-detrended PLP plasma densities and neutral density residuals are shown in the 20:00–22:00 LT sector. The neutral densities exhibit wave-4 periodicity. Three of the maxima coincide with maxima in the plasma density. The deep minimum in plasma density between 300° and 360° coincides with a similar deep minimum in neutral density.

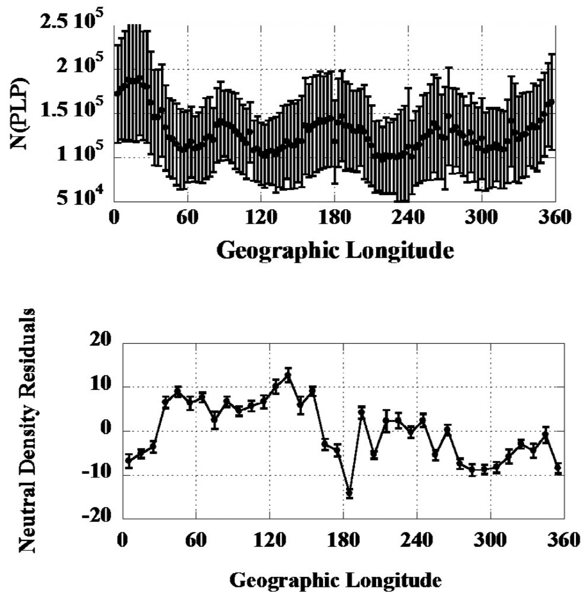

Figure 6. Altitude-detrended PLP plasma densities and neutral density residuals are shown in the 10:00–12:00 LT sector. The plasma densities exhibit wave-4 periodicity which is not matched by the neutrals.

may exhibit a oscillation at the local time precession rate of the satellite (or some fraction of it). Nevertheless, from these plots we can glean information on the nonmigrating tidal structure on the order of 28 days. As the nonmigrating tides are highly variable with season, this provides an attractive alternative to using data from an entire 12 h local time precession period (~161 days for the GRACE satellite).

[19] Figures 5 and 6 show the neutral density residuals resulting from this analysis, together with the detrended PLP densities for local time sectors 20:00–22:00 LT and 10:00–12:00 LT, respectively.

4. Discussion

[20] The average detrended plasma densities shown in Figures 3 and 4 exhibit occasional periodic structures strongly suggestive of tides. These periodicities are most evident in Figure 3 (bottom left), in which four waves appear. The same four-wave structure appears in Figure 3 (middle left), where the IRI model also shows four waves. Similar four-wave periodicity has been shown in DMSP F13 ion data [*Ren et al.*, 2008; *Huang et al.*, 2010], CHAMP electron densities [*Lühr et al.*, 2007; *Pedatella et al.*, 2008] and in Total Electron Content (TEC) data [*Lin et al.*, 2007; *Scherliess et al.*, 2008; *Wan et al.*, 2008; *Pancheva and Mukhtarov*, 2010] and others. The longitudinal distributions of maxima and minima shown in Figure 3 coincide with those in the FUV observations [*Immel et al.*, 2006], in agreement with predictions of the Global Scale Wave Model (GSWM) [*Hagan et al.*, 2001; *Hagan and Forbes*, 2002, 2003]. As discussed by *Pedatella et al.* [2008] and others, the DE3 tide which appears as a wave-4 structure is dominant most of the year, including the June solstice period. It should be noted that the waves in the PLP data appear in the unfiltered plasma observations. Aside from the detrending described above, the plasma data have not been processed to extract wave modes. These tidal structures are dominant during this period, thus the periodicity appears as a macroscopic feature of the ionosphere, creating plasma density variations up to 35% (see Figure 3, bottom left). This sets our analysis apart from previous studies of this phenomenon.

[21] Starting from dawn, shown in Figure 3 (top left), the detrended plasma data show a two-wave structure that evolves into a four-wave pattern over the following 6 h of local time. From 14:00 LT the pattern becomes less clear with 2 clear maxima and possibly 3 smaller maxima evident. Note that the data show clear differences from the IRI model in which periodicity is also seen at 08:00–10:00 LT. In general, the observed plasma density is lower than predicted by the model. In addition, the observed wave features deviate from the model beginning at 10:00 LT. As IRI is an empirical model of ionosphere, the lack of wave-4 periodicity in Figure 3 in the IRI traces shows that our results represent a new ionospheric phenomenon.

[22] In the nighttime ionosphere it is considerably more difficult to discern periodic structure. Fluctuations appear at 18:00–20:00 LT in Figure 4 (top left) as well as at 22:00–24:00 LT and 00:00–02:00 LT, but they appear irregular. Shown on a larger scale, the fluctuations show some periodicity, but tidal structures are not obvious. It is possible that these represent interference due to multiple tidal frequencies, but we have not yet attempted to filter the data to determine if this is the case. It should also be noted that the C/NOFS orbital inclination of 13° may exclude a part of the equatorial anomalies where tidal features are often detected [*England et al.*, 2006; *Liu and Watanabe*, 2008; *Lühr et al.*, 2007]. However, in general the equatorial anomalies are weak during this extremely quiet solar minimum period. A two-wave pattern emerges toward dawn (04:00–06:00 LT) which persists into the dayside (see Figure 3, top left). This is also clear in the IRI model. For the rest of the nightside, IRI results do not display periodic structures.

[23] Wave-4 periodic structures have been observed in other C/NOFS experiments, including the Ion Velocity Meter [*Araujo-Pradere et al.*, 2010] the Vector Electric Field Instrument [*Pfaff et al.*, 2010] and density irregularities in the PLP [*Dao et al.*, 2010]. It is clear that the ionosphere above 400 km during solar minimum is dominated by tidal forces, generally thought to be generated at low altitudes [*Hagan and Forbes*, 2002, 2003]. As in this study, all of these periodic structures detected on C/NOFS are strongest on the dayside. This agrees with the suggestion by *Immel et al.* [2006] that the upward propagating tides reinforce the regular *E* region dynamo which peaks at noon. However, these results are all obtained during a deep solar minimum, when *E* region densities are relatively low. As C/NOFS continues to operate, we will monitor the in situ densities for evidence of wave-4 structures as solar activity increases.

[24] The neutral density residuals obtained from the GRACE accelerometer are shown in Figures 5 and 6 for the dayside and nightside, respectively. Note that the data in Figures 5 and 6 are plotted on different scales. A comparison of the neutrals with ions easily shows that that the tides are not directly coupled. In Figure 5, the plasma averages and neutral density residuals are plotted for the 20:00–22:00 LT bin as functions of longitude. The ions show 3 maxima which coincide with maxima in the neutrals, but there is little variation between 135° and 270°.

[25] In Figure 6 are shown the ion and neutral densities for the 10:00–12:00 LT bin. In this case the ions show wave-4 periodicity while the neutral densities do not. The neutral density residuals have been decomposed into longitudinal wave numbers 1–6 (not shown). There is clear evidence of wave-4 structure in both the 08:00–10:00 LT and 10:00–12:00 LT zones. The Hough modes for DE3 have been compared with the neutral density residuals, and our hypothesis that DE3 waves are present has been confirmed. A full description of the neutral tides will be provided in a separate paper.

[26] Further analysis of the neutral density residuals shows that the results shown in Figure 6 are due to interference from a series of wave modes. The DE3 mode is present, but weaker because of diurnal and semidiurnal tides also present. In general the neutral densities show wave-4 structure most clearly on the nightside. The converse is true of the ion density structures. While all tides have their origin at low altitudes, their subsequent evolution depends on electric fields and winds in the *E* region which affect ion and neutrals in different ways. A causal link between the wave-4 structures and vertical plasma drift has been established [*Fang et al.*, 2009]. We intend to explore this hypothesis in a more comprehensive study.

[27] One feature of our analysis which is apparent in both ions and neutrals is the deep minimum between 300° and 360° on the nightside. This feature corresponds to the BPDs initially identified [*Huang et al.*, 2009]. In the 20:00–22:00 LT sector, the average reduction in density is 85%. While most obvious on the nightside, this minimum appears in all of the local time averages of altitude-detrended ion densities shown in Figures 3–6. It is evident in the IRI values shown in Figures 3 and 4. It is also readily apparent in other studies of ionospheric tides, where it appears as a density decrease [*Fang et al.*, 2009], temperature minimum, or decrease in far ultraviolet (FUV) emissions [*Immel et al.*, 2006]. We showed previously that the BPD is associated with a temperature minimum in the high *F* region at DMSP altitude of 840 km [*Huang et al.*, 2009]. The simultaneity of this minimum in both ions and neutrals on the nightside makes it difficult to separate cause from effect. In situ IVM measurements of meridional drift show a downward-directed velocity in the BPD (R. Stoneback, private communication, 2010) which may suggest ion drag as one possible cause of the neutral density decrease. We believe that ion-neutral coupling is the cause of the simultaneous decrease in ion and neutral density in this location, but cannot postulate a physical mechanism at this time.

5. Conclusion

[28] We have presented an analysis of altitude-detrended plasma densities from the C/NOFS satellite during June 2008. We used the 2007 version of the IRI model to remove altitude and latitude variations from the observed densities. We then averaged the results in bins of local time and longitude. This analysis revealed the presence of wave-4 periodic structures, strongest between 08:00 and 14:00 LT. On the nightside, the periodicity is much weaker, but there is a persistent deep minimum in plasma density at approximately 330°.

[29] We analyzed the neutral density variations from the GRACE satellite during the same period, removing altitude variations and restricting the data to 13° in latitude from the equator, similar to the C/NOFS orbit. We averaged the density residuals in similar local time and longitude bins as for the ion densities. The results exhibit wave-4 periodicity, strongest on the nightside. This is the converse of the ionospheric periodic structures which are strongest on the dayside.

[30] We conclude that periodic structures in both ion and neutral densities are probably generated by tides at low altitudes. However, their subsequent evolution from their common source results in a decoupling of the structures at *F* layer altitudes. One striking exception is the large decrease in density which is seen in both ions and neutrals at 330° on the nightside. We believe this to be the result of ion-neutral coupling, but a mechanism to create this density decrease is beyond the scope of this report.

[31] **Acknowledgments.** The C/NOFS mission is supported by the Air Force Research Laboratory, the Department of Defense Space Test Program, NASA, the Naval Research Laboratory, and the Aerospace Corporation. This research was supported by the Air Force Office of Scientific Research, Task 2301SDA5.

References

Araujo-Pradere, E. A., D. N. Anderson, M. Fedrizzi, and R. Stoneback (2010), Determining the daytime, equatorial ionospheric electron densities associated with the observed, 4-cell longitude patterns in E × B drift velocities, Abstract SA41C-06 presented at 2010 Fall Meeting, AGU, San Francisco, Calif., 13–17 Dec.

Bilitza, D., and B. W. Reinisch (2008), International Reference Ionosphere 2007: Improvements and new parameters, *Adv. Space Res.*, *42*(4), 599–609, doi:10.1016/j.asr.2007.07.048.

Bruinsma, S., D. Tamagnan, and R. Biancale (2004), Atmospheric densities derived from CHAMP/STAR accelerometer observations, *Planet. Space Sci.*, *52*, 297–312, doi:10.1016/j.pss.2003.11.004.

Chapman, S., and R. D. Lindzen (1970), *Atmospheric Tides*, D. Reidel, Dordrecht, Netherlands.

Dao, E. V., M. C. Kelley, J. M. Retterer, O. de La Beaujardière, Y. Su, and P. A. Roddy (2010), Observations and simulation of equatorial irregularities at solar min, Abstract SA51B-1622 presented at 2010 Fall Meeting, AGU, San Francisco, Calif., 13–17 Dec.

de La Beaujardière, O., et al. (2004), C/NOFS: A mission to forecast scintillations, *J. Atmos. Sol. Terr. Phys.*, *66*, 1573–1591, doi:10.1016/j.jastp.2004.07.030.

England, S. L., T. J. Immel, E. Sagawa, S. B. Henderson, M. E. Hagan, S. B. Mende, H. U. Frey, C. M. Swenson, and L. J. Paxton (2006), Effect of atmospheric tides on the morphology of the quiet time, postsunset equatorial ionospheric anomaly, *J. Geophys. Res.*, *111*, A10S19, doi:10.1029/2006JA011795.

Fang, T.-W., H. Kil, G. Millward, A. D. Richmond, J.-Y. Liu, and S.-J. Oh (2009), Causal link of the wave-4 structures in plasma density and vertical plasma drift in the low-latitude ionosphere, *J. Geophys. Res.*, *114*, A10315, doi:10.1029/2009JA014460.

Hagan, M. E., and J. M. Forbes (2002), Migrating and nonmigrating diurnal tides in the middle and upper atmosphere excited by tropospheric latent heat release, *J. Geophys. Res.*, *107*(D24), 4754, doi:10.1029/2001JD001236.

Hagan, M. E., and J. M. Forbes (2003), Migrating and nonmigrating semidiurnal tides in the upper atmosphere excited by tropospheric latent heat release, *J. Geophys. Res.*, *108*(A2), 1062, doi:10.1029/2002JA009466.

Hagan, M. E., R. G. Roble, and J. Hackney (2001), Migrating thermospheric tides, *J. Geophys. Res.*, *106*, 12,739–12,752, doi:10.1029/2000JA000344.

Huang, C.-S., F. J. Rich, O. de La Beaujardière, and R. A. Heelis (2010), Longitudinal and seasonal variations of the equatorial ionospheric ion density and eastward drift velocity in the dusk sector, *J. Geophys. Res.*, *115*, A02305, doi:10.1029/2009JA014503.

Huang, C. Y., F. A. Marcos, P. A. Roddy, M. R. Hairston, W. R. Coley, C. Roth, S. Bruinsma, and D. E. Hunton (2009), Broad plasma decreases in the equatorial ionosphere, *Geophys. Res. Lett.*, *36*, L00C04, doi:10.1029/2009GL039423.

Immel, T. J., E. Sagawa, S. L. England, S. B. Henderson, M. E. Hagan, S. B. Mende, H. U. Frey, C. M. Swenson, and L. J. Paxton (2006), Control of equatorial ionospheric morphology by atmospheric tides, *Geophys. Res. Lett.*, *33*, L15108, doi:10.1029/2006GL026161.

Lin, C. H., C. C. Hsiao, J. Y. Liu, and C. H. Liu (2007), Longitudinal structure of the equatorial ionosphere: Time evolution of the four-peaked EIA structure, *J. Geophys. Res.*, *112*, A12305, doi:10.1029/2007JA012455.

Lindzen, R. S., and S. Chapman (1969), Atmospheric tides, *Space Sci. Rev.*, *10*, 3–188.

Liu, H., and S. Watanabe (2008), Seasonal variation of the longitudinal structure of the equatorial ionosphere: Does it reflect tidal influences from below?, *J. Geophys. Res.*, *113*, A08315, doi:10.1029/2008JA013027.

Lühr, H., K. Häusler, and C. Stolle (2007), Longitudinal variation of *F* region electron density and thermospheric zonal wind caused by atmospheric tides, *Geophys. Res. Lett.*, *34*, L16102, doi:10.1029/2007GL030639.

Pancheva, D., and P. Mukhtarov (2010), Strong evidence for the tidal control on the longitudinal structure of the ionospheric *F* region, *Geophys. Res. Lett.*, *37*, L14105, doi:10.1029/2010GL044039.

Pedatella, N. M., J. M. Forbes, and J. Oberheide (2008), Intra-annual variability of the low-latitude ionosphere due to nonmigrating tides, *Geophys. Res. Lett.*, *35*, L18104, doi:10.1029/2008GL035332.

Pfaff, R. F., H. Freudenreich, J. H. Klenzing, D. E. Rowland, M. C. Liebrecht, K. R. Bromund, and P. A. Roddy (2010), Persistent longitudinal variations of plasma density and DC electric fields in the low latitude ionosphere observed with probes on the C/NOFS satellite, Abstract SA41C-03 presented at 2010 Fall Meeting, AGU, San Francisco, Calif., 13–17 Dec.

Ren, Z., W. Wan, L. Liu, B. Zhao, Y. Wei, X. Yue, and R. A. Heelis (2008), Longitudinal variations of electron temperature and total ion den-

sity in the sunset equatorial topside ionosphere, *Geophys. Res. Lett.*, *35*, L05108, doi:10.1029/2007GL032998.
Scherliess, L., D. C. Thompson, and R. W. Schunk (2008), Longitudinal variability of low-latitude total electron content: Tidal influences, *J. Geophys. Res.*, *113*, A01311, doi:10.1029/2007JA012480.
Sutton, E. K. (2009), Normalized force coefficients for satellites with elongated shapes, *J. Spacecr. Rockets*, *46*(1), 112–116, doi:10.2514/1.40940.
Sutton, E. K., J. M. Forbes, and R. S. Nerem (2005), Global thermospheric neutral density and wind response to the severe 2003 geomagnetic storms from CHAMP accelerometer data, *J. Geophys. Res.*, *110*, A09S40, doi:10.1029/2004JA010985.
Wan, W., L. Liu, X. Pi, M.-L. Zhang, B. Ning, J. Xiong, and F. Ding (2008), Wavenumber-4 patterns of the total electron content over the low latitude ionosphere, *Geophys. Res. Lett.*, *35*, L12104, doi:10.1029/2008GL033755.

S. H. Delay, Institute for Scientific Research, 400 St. Clement's Hall, Boston College, 140 Commonwealth Ave., Chestnut Hill, MA 02467, USA.
C. Y. Huang, P. A. Roddy, and E. K. Sutton, Space Vehicles Directorate, Air Force Research Laboratory, 29 Randolph Rd., Hanscom AFB, MA 01731-3010, USA. (afrl.rvb.pa@hanscom.af.mil)

DISTRIBUTION LIST

DTIC/OCP 8725 John J. Kingman Rd, Suite 0944 Ft Belvoir, VA 22060-6218	1 cy
AFRL/RVIL Kirtland AFB, NM 87117-5776	2 cys
Official Record Copy AFRL/RVBXP/Cheryl Huang	1 cy

This page intentionally left blank.